

Cite this: DOI: 10.1039/c3dt50496d

Visible light-harvesting *trans* bis(alkylphosphine) platinum(II)-alkynyl complexes showing long-lived triplet excited states as triplet photosensitizers for triplet–triplet annihilation upconversion†

Lianlian Liu,^a Dandan Huang,^a Sylvia M. Draper,^b Xiuyu Yi,^a Wanhua Wu^a and Jianzhang Zhao^{*a}

Symmetric and asymmetric linear *trans*-bis(tributylphosphine) Pt(II) bis(acetylide) complexes with functionalized aryl alkynyl ligands (coumarin, naphthalimide and phenyl acetylides) were prepared, which show enhanced absorption in the visible region (molar absorption coefficients up to 76 800 M⁻¹ cm⁻¹ at 459 nm) and long-lived triplet excited states (up to 139.9 μs). At room temperature, the naphthalimide acetylide–phenyl acetylide complex (**Pt-4**) shows dual emission (fluorescence–phosphorescence), whereas other complexes show only fluorescence emission. The triplet excited states of the complexes were studied with nanosecond time-resolved transient difference absorption spectroscopy and DFT calculations on the spin density surface. The complexes were used as triplet photosensitizers for ratiometric O₂ sensing, as well as triplet–triplet annihilation (TTA) upconversion (upconversion quantum yield up to 27.2%). The TTA upconversion of the complexes requires triplet acceptors with different T₁ state energy levels and was studied with nanosecond time-resolved emission spectroscopy. Our results are useful for designing new Pt(II) complexes that show strong absorption of visible light and long-lived triplet excited states, as well as for the application of these complexes as triplet photosensitizers for O₂ sensing, photocatalysis and TTA upconversion.

Received 23rd February 2013,
Accepted 3rd April 2013

DOI: 10.1039/c3dt50496d

www.rsc.org/dalton

Introduction

Pt(II) complexes have attracted much attention due to their applications in photocatalysis,^{1,2} photovoltaics,³ non-linear optics and molecular probes,^{4–8} and more recently in triplet–triplet annihilation upconversions.^{9–12} In most of these applications, the absorption of visible light and long-lived triplet excited states is crucial. However, conventional Pt(II) complexes usually show *weak* absorption in the visible region and short T₁ state lifetimes (less than 10 μs).^{13–18}

Linear bis(alkylphosphine) Pt(II) acetylide complexes are in particular interesting because their molecular structure and their photophysical properties are readily tunable by using different acetylide ligands.^{3,4,14,19–21} These complexes have

been used for non-linear optics and photovoltaics.^{3–8} However, most of the reported linear phosphine Pt(II) acetylide complexes show weak absorption in the visible region and short-lived triplet excited states (at RT),^{3,4,19–21} which are detrimental for the application of these complexes as triplet photosensitizers. To the best of our knowledge, no linear bis(alkylphosphine) Pt(II) acetylide complexes have been used as triplet photosensitizers for luminescent oxygen (O₂) sensing and very few were used for TTA upconversion.^{9–12,21c,22}

In order to address these challenges, herein we used aryl acetylides to synthesis linear bis(alkylphosphine) Pt(II) bis(acetylide) complexes, *i.e.* naphthalimide and coumarin acetylides, to induce strong absorption of visible light and long-lived triplet excited states. The photophysical properties of the complexes were studied with UV-vis absorption and luminescence spectra. The triplet excited states of the complexes were studied with nanosecond time-resolved transient difference absorption spectroscopy and DFT calculations on the spin density surfaces. These studies demonstrate that the complexes show strong absorption of visible light and long-lived triplet excited states such that the complexes could be used as triplet photosensitizers for luminescent oxygen (O₂) sensing

^aState Key Laboratory of Fine Chemicals, School of Chemical Engineering, Dalian University of Technology, E 208 Western Compus, 2 Ling-Gong Road, Dalian 116012, P. R. China. E-mail: zhaojzh@dlut.edu.cn; http://finechem.dlut.edu.cn/photochem

^bSchool of Chemistry, University of Dublin, Trinity College, Dublin 2, Ireland

†Electronic supplementary information (ESI) available: The synthesis and the structure characterization data of the Pt(II) complexes; the details of TTA upconversion and DFT calculation information. See DOI: 10.1039/c3dt50496d

and TTA upconversion. The performance of the triplet photosensitizers was much improved compared to the conventional Pt(II) complexes that show weak absorption of visible light and short-lived triplet excited states.

Experimental

Materials and reagents

All the chemicals were analytically pure and were used as received. Solvents were dried and distilled before use.

Analytical measurements

NMR spectra were recorded on a 400 MHz Varian Unity Inova spectrophotometer (with TMS as the standard). Mass spectra were recorded with a Q-TOF Micro MS spectrometer. UV-vis absorption spectra were measured with an Agilent 8453 UV-vis spectrophotometer. Fluorescence spectra were recorded on a Shimadzu RF-5301PC spectrofluorometer. Upconversion was carried out on a modified Sanco 970 CRT spectrofluorometer. Phosphorescence quantum yields were measured with [Ru(dmb)₃(PF₆)₂] as the standard ($\Phi = 0.073$ in acetonitrile. *dmb* = 4,4'-dimethyl-2,2'-bipyridine). Luminescence lifetimes were measured on an OB920 luminescence lifetime spectrometer (Edinburgh Instruments, UK) and an FLS920 spectrofluorometer (Edinburgh Instruments, UK). Complex **3** was synthesised with a microwave reaction (MCR-3 microwave reactor). The temperature of the reaction mixture was kept at 75 °C.

Complex **1**^{3,8,14}

Under an Ar atmosphere, phenylacetylene (13.8 mg, 0.135 mmol) was added to the solution of *cis*-Pt[P(*n*-Bu)₃]₂Cl₂ (100.0 mg, 0.149 mmol) in diethylamine (NHET₂) (6 mL), the flask was evacuated and back-filled with Ar several times. The mixture was heated at 45 °C and stirred for 6 h. After complete consumption of the starting material, the solvents were evaporated under reduced pressure, and the crude product was further purified using column chromatography (silica gel, CH₂Cl₂-hexane = 2 : 3, v/v) to give **1** as a light yellow solid (75.2 mg), yield: 75.7%. ¹H NMR (400 MHz, CDCl₃): 7.25–7.18 (m, 4H), 7.14–7.11 (m, 1H), 2.03–1.99 (m, 12H), 1.57–1.54 (m, 12H), 1.49–1.40 (m, 12H), 0.92 (t, 18H, *J* = 7.3 Hz).

Compound **2**

Bromine (367.6 mg, 2.3 mmol) was added *via* a syringe to a solution of coumarin (500.0 mg, 2.3 mmol) in acetic acid (13 mL) in 40 min. The mixture was stirred at RT for 2 h. Then Na₂S₂O₃ (570.8 mg, 2.3 mmol) was added and the mixture was stirred at RT for 10 min. The solid was collected with filtration. After washing with acetic acid and water, the residue was dried under vacuum. The crude product was further purified using column chromatography (silica gel, CH₂Cl₂-petroleum ether = 3 : 2, v/v) to give **2** as a light yellow solid (613.1 mg), yield: 90.0%. ¹H NMR (400 MHz, CDCl₃): 7.88 (s, 1H), 7.20 (d, 1H, *J* = 8.0 Hz), 6.58 (d, 1H, *J* = 8.0 Hz), 6.48 (s, 1H), 3.44–3.39 (m, 4H),

1.19 (t, 6H, *J* = 8.0 Hz). ESI-HRMS: calcd [(C₁₃H₁₄BrNO₂ + H)⁺] *m/z* = 296.0286, found *m/z* = 296.0270.

Compound **3**

Compound **2** (300.0 mg, 1.013 mmol), 2-thienylboronic acid (281.8 mg, 2.2 mmol) and K₂CO₃ (608.2 mg, 4.4 mmol) were dissolved in a mixed solvent MeOH-PhCH₃ (3 : 4, v/v, 20 mL), and then Pd(PPh₃)₄ (60.2 mg, 0.052 mmol) was added. The flask was vacuumed and back-filled with Ar several times. The reaction mixture was heated at 75 °C for 30 min in a microwave reactor. Water was added, then the mixture was extracted with CH₂Cl₂ (3 × 50 mL). The organic phase was dried with Na₂SO₄, filtered and the solvent was removed under reduced pressure. The crude product was further purified using column chromatography (silica gel, CH₂Cl₂-petroleum ether = 1 : 1, v/v) to give **3** as a light yellow solid (250.4 mg), yield: 82.4%. ¹H NMR (400 MHz, CDCl₃): 7.88 (s, 1H), 7.66 (d, 1H, *J* = 4.0 Hz), 7.33–7.31 (m, 2H), 7.08 (d, 1H, *J* = 4.0 Hz), 6.61 (d, 1H, *J* = 8.0 Hz), 6.54 (s, 1H), 3.44–3.42 (m, 4H), 1.21 (t, 6H, *J* = 8.0 Hz). ESI-HRMS: calcd [(C₁₇H₁₇SNO₂ + H)⁺] *m/z* = 300.1058, found *m/z* = 300.1044.

Compound **4**

Compound **3** (62.0 mg, 0.21 mmol) was dissolved in a mixed solvent CHCl₃-AcOH (5 mL/5 mL), then NBS (44.2 mg, 0.249 mmol) was added at 0 °C, in three portions at 20 min intervals. The mixture was stirred at RT for 4 h. After addition of water, the mixture was extracted with CH₂Cl₂ (3 × 50 mL). The organic phase was dried with Na₂SO₄, filtered and the solvent was removed under reduced pressure. The crude product was further purified using column chromatography (silica gel, CH₂Cl₂-petroleum ether = 2 : 3, v/v) to give **4** as a light yellow solid (62.1 mg), yield: 78.0%. ¹H NMR (400 MHz, CDCl₃): 7.83 (s, 1H), 7.34–7.33 (m, 2H), 7.03 (s, 1H), 6.62 (d, 1H, *J* = 8.0 Hz), 6.53 (s, 1H), 3.46–3.41 (m, 4H), 1.21 (t, 6H, *J* = 8.0 Hz). ESI-HRMS: calcd [(C₁₇H₁₆SNO₂Br + Na)⁺] *m/z* = 399.9983, found *m/z* = 399.9975.

Compound **5**

Under an Ar atmosphere, Pd(PPh₃)₂Cl₂ (9.3 mg, 0.0132 mmol), PPh₃ (6.9 mg, 0.0264 mmol) and CuI (5.0 mg, 0.0264 mmol) were added to a solution of **4** (50.0 mg, 0.132 mmol) in a mixed solvent of THF-Et₃N (6 mL/2 mL). Trimethylsilylacetylene (64.8 mg, 0.66 mmol) was added *via* a syringe. The mixture was stirred at 70 °C for 8 h. After the addition of water, the mixture was extracted with CH₂Cl₂ (3 × 50 mL). The organic phase was dried with Na₂SO₄, filtered and the solvent was removed under reduced pressure. The crude product was further purified using column chromatography (silica gel, CH₂Cl₂-petroleum ether = 1 : 1, v/v) to give **5** as a dark yellow solid (23.5 mg), yield: 44.7%. ¹H NMR (400 MHz, CDCl₃): 7.86 (s, 1H), 7.47 (d, 1H, *J* = 4.0 Hz), 7.30 (d, 1H, *J* = 12.0 Hz), 7.18 (d, 1H, *J* = 4.0 Hz), 6.60 (d, 1H, *J* = 12.0 Hz), 6.50 (s, 1H), 3.44–3.41 (m, 4H), 1.21 (t, 6H, *J* = 8.0 Hz), 0.25 (s, 9H). ESI-HRMS: calcd [(C₂₂H₂₅SNO₂Si + H)⁺] *m/z* = 396.1454, found *m/z* = 396.1446.

Ligand L-1

K_2CO_3 (207.0 mg, 1.5 mmol) was added to a solution of compound **5** (300.2 mg, 0.77 mmol) in a mixed solvent THF–MeOH (8 mL/4 mL). The mixture was stirred at room temperature for 1.5 h. After the addition of water, CH_2Cl_2 was added to extract the product (3 × 50 mL). The organic phase was dried with Na_2SO_4 , filtered and the solvent was evaporated under reduced pressure. The crude product was further purified using column chromatography (silica gel, CH_2Cl_2 –petroleum ether = 1 : 1, v/v) to give **L-1** as a light red solid (35.6 mg), yield: 87.3%. ^1H NMR (400 MHz, CDCl_3): 7.86 (s, 1H), 7.46 (d, 1H, J = 4.0 Hz), 7.30 (d, 1H, J = 8.0 Hz), 7.22 (d, 1H, J = 4.0 Hz), 6.59 (d, 1H, J = 12.0 Hz), 6.50 (s, 1H), 3.45–3.40 (m, 5H), 1.20 (t, 6H, J = 8.0 Hz). ^{13}C NMR (100 MHz, CDCl_3): 160.6, 155.8, 151.0, 139.3, 137.3, 133.4, 129.3, 124.0, 121.9, 114.0, 109.6, 108.7, 97.2, 82.2, 45.1, 12.7 ppm. ESI-HRMS: calcd $[(\text{C}_{19}\text{H}_{17}\text{SNO}_2 + \text{H})^+]$ m/z = 324.1058, found m/z = 324.1056.

Complex Pt-0

The synthetic procedure is similar to that of **1**, except that naphthalimide acetylene (41.3 mg, 0.124 mmol) was used. The crude product was further purified using column chromatography (silica gel, CH_2Cl_2 –petroleum ether = 1 : 2, v/v) to give **Pt-0** as a light yellow oil (63.2 mg), yield: 52.2%. ^1H NMR (400 MHz, CDCl_3): 8.68 (d, 1H, J = 8.0 Hz), 8.53 (d, 1H, J = 4.0 Hz), 8.40 (d, 1H, J = 8.0 Hz), 7.64–7.62 (m, 1H), 7.54 (d, 1H, J = 8.0 Hz), 4.12–4.03 (m, 2H), 1.97 (t, 12H, J = 4.0 Hz), 1.57–1.56 (m, 12H), 1.21–1.41 (m, 21H), 0.83–0.89 (m, 24H). ^{13}C NMR (100 MHz, CDCl_3): 165.0, 164.7, 133.8, 133.3, 131.3, 131.2, 128.9, 128.7, 126.2, 123.1, 118.8, 102.2, 100.6, 44.2, 38.1, 30.9, 29.8, 28.9, 26.3, 24.5, 24.4, 24.2, 23.2, 22.3, 22.2, 14.2, 14.0, 10.8 ppm. MALDI-HRMS: calcd $[(\text{C}_{46}\text{H}_{76}\text{NO}_2\text{PtCl} + \text{H})^+]$ m/z = 967.4766, found m/z = 967.4691.

Compound Pt-1

Under an Argon atmosphere, compound **1** (50.1 mg, 0.068 mmol) and **L-1** (22.0 mg, 0.068 mmol) were dissolved in a mixed solvent THF–Et₂NH (3 mL/3 mL). The flask was evacuated and back-filled with Ar several times, and then CuI (2.9 mg, 0.015 mmol) was added, the mixture was stirred at RT for 30 min. Deionized water was used to quench the reaction mixture, CH_2Cl_2 was added to extract the product (3 × 50 mL). The organic phase was dried with Na_2SO_4 , filtered and the solvent was removed under reduced pressure. The crude product was further purified using column chromatography (silica gel, CH_2Cl_2 –petroleum ether = 1 : 2, v/v) to give **Pt-1** as a dark yellow solid (29.8 mg), yield: 42.9%. ^1H NMR (400 MHz, CDCl_3): 7.75 (s, 1H), 7.49 (s, 1H), 7.30–7.11 (m, 6H), 6.81 (d, 1H, J = 4.0 Hz), 6.58 (d, 1H, J = 8.0 Hz), 6.51 (s, 1H), 3.44–3.39 (m, 4H), 2.11 (t, 12H, J = 8.0 Hz), 1.6 (s, 12H), 1.49–1.46 (m, 12H), 1.2 (t, 6H, J = 8.0 Hz), 0.92 (t, 18H, J = 8.0 Hz). ^{13}C NMR (100 MHz, CDCl_3): 160.6, 155.4, 150.3, 135.5, 134.1, 130.9, 130.3, 129.2, 128.7, 128.0, 125.3, 125.0, 117.0, 115.4, 109.3, 109.2, 107.8, 101.6, 97.3, 65.7, 45.0, 32.1, 30.7, 29.9, 29.5, 26.5, 24.6, 24.1, 23.9, 22.9, 19.4, 14.0, 12.7 ppm. MALDI-HRMS:

calcd $[(\text{C}_{51}\text{H}_{75}\text{NO}_2\text{P}_2\text{SPT})^+]$ m/z = 1022.4642, found m/z = 1022.4685.

Compound Pt-2

The synthetic procedure is similar to that of **Pt-1**, except that **Pt-0** (65.7 mg, 0.068 mmol) was used. The crude product was further purified using column chromatography (silica gel, CH_2Cl_2 –petroleum ether = 1 : 1, v/v) to give **Pt-2** as a dark yellow solid (43.9 mg), yield: 51.5%. ^1H NMR (400 MHz, CDCl_3): 8.77 (d, 1H, J = 8.0 Hz), 8.57 (d, 1H, J = 4.0 Hz), 8.44 (d, 1H, J = 8.0 Hz), 7.78 (s, 1H), 7.69–7.66 (m, 1H), 7.6 (d, 1H, J = 8.0 Hz), 7.5 (d, 1H, J = 4.0 Hz), 7.3 (d, 1H, J = 12.0 Hz), 6.85 (d, 1H, J = 4.0 Hz), 6.64–6.55 (m, 2H), 4.08–4.14 (m, 2H), 3.44–3.40 (m, 4H), 2.09 (t, 12H, J = 8.0 Hz), 1.64 (s, 12H), 1.48–1.23 (m, 27H), 0.95–0.88 (m, 24H). ^{13}C NMR (100 MHz, CDCl_3): 165.1, 164.8, 160.6, 155.4, 150.3, 135.7, 134.4, 134.0, 133.5, 132.2, 131.2, 131.0, 128.7, 126.0, 125.0, 122.9, 118.5, 115.2, 109.3, 109.1, 97.3, 94.5, 70.6, 46.0, 45.0, 44.2, 38.1, 32.0, 30.9, 29.8, 28.9, 26.6, 24.5, 24.2, 23.2, 22.8, 14.2, 14.0, 12.6, 10.8, 8.7 ppm. MALDI-HRMS: calcd $[(\text{C}_{65}\text{H}_{92}\text{N}_2\text{O}_4\text{P}_2\text{SPT})^+]$ m/z = 1253.5901, found m/z = 1253.5989.

Compound Pt-3

The synthetic procedure is similar to that of **1**, except that **L-1** (40.0 mg, 0.008 mmol) was used. The crude product was further purified by column chromatography (silica gel, CH_2Cl_2 –petroleum ether = 2 : 1, v/v) to give **Pt-3** as a dark yellow solid (59.8 mg), yield: 38.7%. ^1H NMR (400 MHz, CDCl_3): 7.75 (s, 2H), 7.5 (d, 2H, J = 4.0 Hz), 7.28 (d, 2H, J = 12.0 Hz), 6.81 (d, 2H, J = 4.0 Hz), 6.58 (d, 2H, J = 4.0 Hz), 6.52 (s, 2H), 3.43–3.4 (m, 8H), 2.11 (t, 12H, J = 4.0 Hz), 1.72–1.6 (m, 12H), 1.51–1.48 (m, 12H), 1.2 (t, 12H, J = 8.0 Hz), 0.93 (t, 18H, J = 8.0 Hz). MALDI-HRMS: calcd $[(\text{C}_{62}\text{H}_{86}\text{N}_2\text{O}_4\text{P}_2\text{S}_2\text{Pt} + \text{H})^+]$ m/z = 1244.5230, found m/z = 1244.5228.

Compound Pt-4

The synthetic procedure is similar to that of **Pt-1**, except that **Pt-0** (20.0 mg, 0.0207 mmol) and phenylacetylene (2.5 mg, 0.025 mmol) were used. The crude product was further purified using column chromatography (silica gel, CH_2Cl_2 –petroleum ether = 1 : 2, v/v) to give **Pt-4** as a light yellow oil (15.0 mg), yield: 70.1%. ^1H NMR (400 MHz, CDCl_3): 7.78 (d, 1H, J = 8.0 Hz), 8.56 (d, 1H, J = 8.0 Hz), 8.44 (d, 1H, J = 8.0 Hz), 7.69–7.65 (m, 1H), 7.6 (d, 1H, J = 8.0 Hz), 7.30–7.22 (m, 4H), 7.15–7.12 (m, 1H), 4.17–4.06 (m, 2H), 2.13 (t, 12H, J = 4.0 Hz), 1.64–1.63 (m, 12H), 1.48–1.30 (m, 21H), 0.89 (t, 24H, J = 8.0 Hz). ^{13}C NMR (100 MHz, CDCl_3): 165.2, 164.9, 134.2, 133.7, 132.3, 131.3, 131.0, 128.7, 128.1, 126.1, 125.3, 118.5, 110.0, 108.1, 106.6, 44.2, 38.2, 31.0, 29.9, 28.9, 26.6, 24.6, 24.3, 24.1, 23.3, 14.3, 14.0, 10.9 ppm. MALDI-HRMS: calcd $[(\text{C}_{54}\text{H}_{81}\text{NO}_2\text{P}_2\text{Pt} + \text{H})^+]$ m/z = 1033.5469, found m/z = 1033.5457.

Compound Pt-5

The synthetic procedure is similar to that of **1**, except that phenylacetylene (20.0 mg, 0.2 mmol) was used. The crude

product was further purified using column chromatography (silica gel, CH₂Cl₂–petroleum ether = 2 : 3, v/v) to give **Pt-5** as a white solid (120.3 mg), yield: 75.0%. ¹H NMR (400 MHz, CDCl₃): 7.26 (d, 4H, *J* = 4.0 Hz), 7.17 (t, 4H, *J* = 8.0 Hz), 7.12–7.10 (m, 2H), 2.13 (t, 12H, *J* = 4.0 Hz), 1.61–1.60 (m, 12H), 1.47–1.41 (m, 12H), 0.90 (t, 18H, *J* = 8.0 Hz). TOF MS: calcd ([C₄₀H₆₄P₂Pt]⁺) *m/z* = 801.4131, found *m/z* = 801.5756.

Triplet–triplet annihilation upconversion

A diode pumped solid state (DPSS) continuous laser (445 nm) was used as an excitation source for the upconversion. The diameter of the 445 nm laser spot is *ca.* 3 mm. The power of the laser beam was measured with a VLP-2000 pyroelectric laser power meter. For the upconversion experiments, the mixed solution of the complexes (triplet photosensitizers) and 9,10-diphenylanthracene (DPA) or perylene was degassed with N₂ for at least 15 min. The upconverted fluorescence of DPA was observed with a CRT 920 spectrofluorometer. In order to repress the scattered laser, a small black box was put behind the fluorescent cuvette to trap the laser beam.

The upconversion quantum yields (Φ_{UC}) were determined with the prompt fluorescence of coumarin-6 as the luminescence quantum yield standard ($\Phi_F = 78\%$ in ethanol). The upconversion quantum yields were calculated using eqn (1),^{9,23–26} where Φ_{UC} , A_{sam} , I_{sam} and η_{sam} represent the quantum yield, absorbance, integrated photoluminescence intensity and the refractive index of the solvents (where the subscript “std” stands for the standard used in the measurement of the quantum yield and “sam” for the samples to be measured). The equation is multiplied by a factor of 2 in order to set the maximum quantum yield to unity. All these data were independently measured three times (with different sample solutions).

$$\Phi_{UC} = 2\Phi_{std} \left(\frac{A_{std}}{A_{sam}} \right) \left(\frac{I_{sam}}{I_{std}} \right) \left(\frac{\eta_{sam}}{\eta_{std}} \right)^2 \quad (1)$$

The CIE coordinates (*x*, *y*) of the emission of the sensitizers alone and the emission of the upconversion were derived from the emission spectra with the software of CIE color Matching Linear Algebra.

DFT calculations

Density functional theory (DFT) calculations were used for optimization of both singlet states and triplet states. The energy level of the T₁ state (energy gap between S₀ state and T₁ state) was calculated with time-dependent DFT (TDDFT), based on the optimized singlet ground state geometries (S₀ state). All the calculations were performed with Gaussian 09W.²⁷

Results and discussion

Design and synthesis of complexes

We have previously used coumarin for preparation of Pt(II) complexes.²⁸ However, coumarin–Pt(II) complexes show

absorption in the UV/blue region, and their molar extinction coefficient is not large. Thiophene units are often used to extend π -conjugation.^{29,30} Herein we attached the thiophene moiety to a coumarin unit to enhance the UV-Vis absorption. The ethenyl bond is attached on the thiophene unit therefore we envisaged an electronic communication between the Pt(II) center and the coumarin unit (Scheme 1). Furthermore, we also used naphthalimide (NI) for accessing the long-lived ³IL excited state.^{31–33} The two acetylde ligands in the complex molecules are the same (**Pt-3**) or different (**Pt-1**, **Pt-2** and **Pt-4**). **Pt-0** was prepared as a model complex.

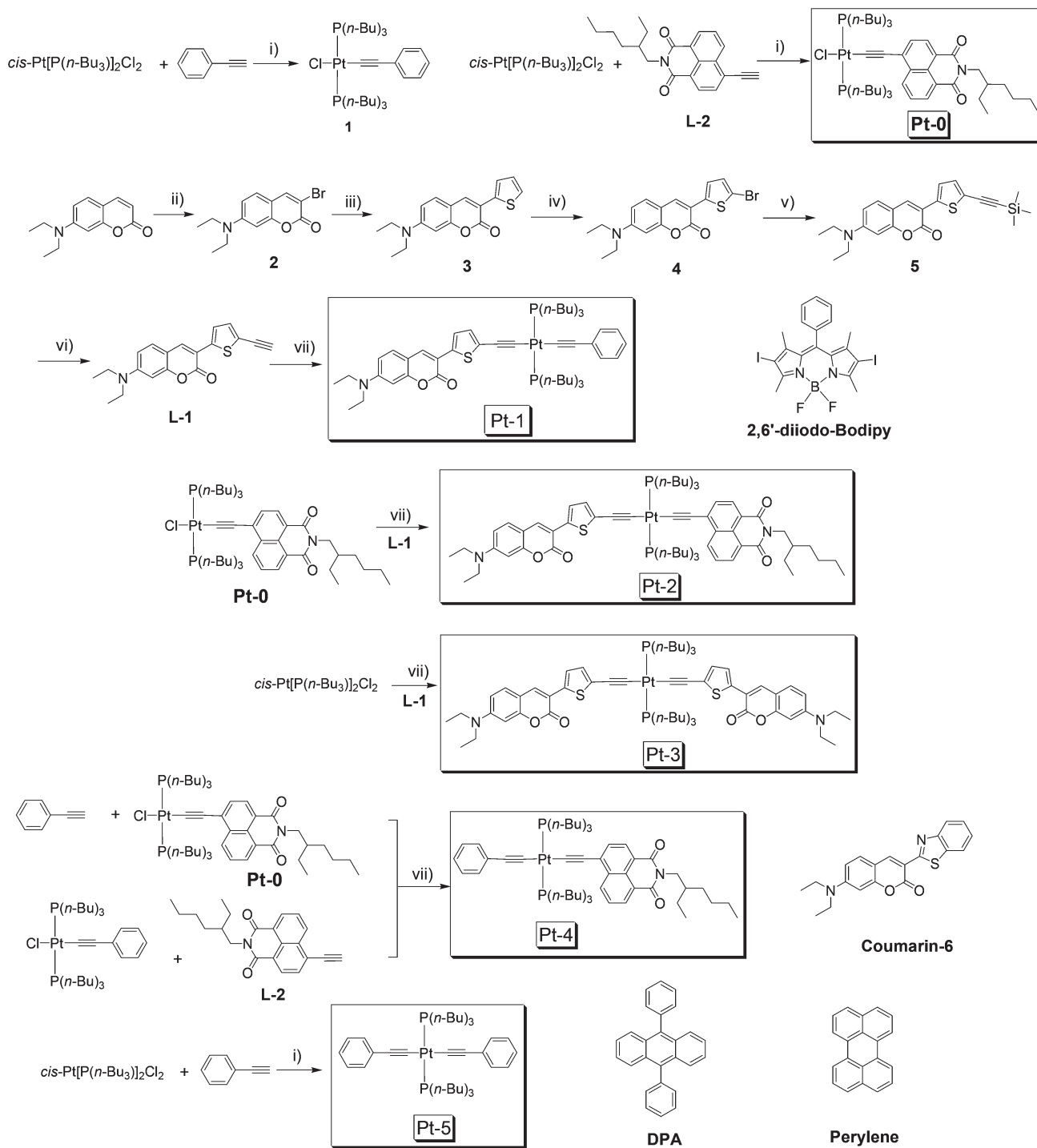
The preparation of the coumarin ligands is based on the Pd(0) catalyzed Suzuki and Sonogashira coupling reactions. The preparation of the NI acetylde ligand was based on the reported method. We observed a unique fluorescence–phosphorescence dual emission for **Pt-4**. In order to rule out any impurity, **Pt-4** was prepared using two different procedures (Scheme 1). All the complexes were obtained with moderate to satisfactory yields.

Absorption and emission spectra

The UV-vis absorption of the complexes and the ligands was studied (Fig. 1). The acetylde ligand **L-1** gives absorption maxima in the visible region (436 nm with 19 100 M^{−1} cm^{−1}). On metalation of the acetylde ligand (**Pt-1**), the absorption band moves bathochromically to 449 nm (33 700 M^{−1} cm^{−1}). For the Pt(II) complex that contains two thienyl coumarin units, the absorption is very strong at 459 nm (76 800 M^{−1} cm^{−1}). Complexes with NI acetylde show similar absorption maxima.

The luminescence properties of the complexes were studied (Fig. 2). All the complexes give emission at *ca.* 500 nm, except **Pt-5**, which was non-luminescent (see ESI† for details). The Stokes shifts of the complexes were small compared to typical phosphorescent transition metal complexes.^{16,34–37} Furthermore, we found that the luminescence intensity of **Pt-1**, **Pt-2** and **Pt-3** was not sensitive to oxygen (O₂). Usually the phosphorescence of transition metal complexes can be substantially quenched by O₂. The luminescence lifetime of the emission at *ca.* 500 nm was determined to be in the range of a few nanoseconds (Table 1). Based on these results, we conclude that the luminescence bands at 500 nm for complexes **Pt-1–Pt-3** are due to fluorescence, not phosphorescence, which is different from the *N^N* Pt(II) bis(acetylde) complexes which are usually phosphorescent.^{18,38–41}

Two emission bands were observed for **Pt-4** (Fig. 2d), one fluorescence emission band at 469 nm and the other emission band at 630 nm. The band at 630 nm is highly sensitive to the presence of O₂, and the luminescence lifetime was determined as 278.6 μ s (in toluene). These data and the large Stokes shift (49 020 cm^{−1}) indicated that the emission at 630 nm can be attributed to phosphorescence. The lifetime of the emission band at 469 nm is 1.0 ns. Thus the emission band can be assigned as fluorescence. In order to validate that these dual emissive features of **Pt-4** were not due to fluorescent impurities, the complex was prepared with two different procedures,



Scheme 1 Synthesis of the complexes **Pt-0**, **Pt-1**, **Pt-2**, **Pt-3**, **Pt-4** and **Pt-5**. Please note **Pt-4** was prepared by two different methods to rule out the presence of impurities in the product. (i) NH_4Et_2 , 45 °C, Ar, 8 h; (ii) Br_2 , AcOH, r.t., 3 h; (iii) 2-thienylboric acid, K_2CO_3 , $\text{Pd(PPh}_3)_4$, MeOH–PhCH₃, Ar, 75 °C, 30 min, microwave reactor; (iv) NBS, CHCl_3 –AcOH, r.t., 4 h; (v) trimethylsilylacetylene, $\text{Pd(PPh}_3)_2\text{Cl}_2$, PPh_3 , CuI, NEt_3 , Ar, reflux, 8 h; (vi) K_2CO_3 , THF–MeOH, r.t., 1.5 h; (vii) THF– HNEt_2 , CuI, Ar, r.t., 30 min.

but the same emission bands were observed. The luminescence lifetimes of the precursors of **Pt-4** also support this conclusion (Table 1).

Dual emission was also observed for **Pt-0** (458 nm and 628 nm) but with much weaker phosphorescence than the

fluorescence. It should be noted that fluorescence–phosphorescence dual emissive transition metal complexes are rare.^{22,42–44} Such complexes are interesting for photophysical studies, as well as for applications in ratiometric oxygen (O_2) sensing.

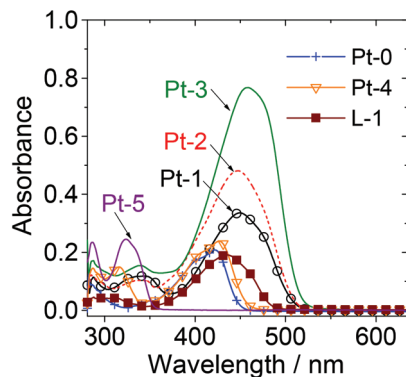


Fig. 1 UV-Vis absorption spectra of the Pt(II) complexes and ligand **L-1**. $c = 1.0 \times 10^{-5}$ M in toluene, 25 °C.

77 K emission spectra

The photoluminescence of the complexes at 77 K was studied (Fig. 3). The emission bands of **Pt-1**, **Pt-2** and **Pt-3** become structured, no phosphorescence bands were observed (see ESI† for details). The luminescence lifetimes of **Pt-1**, **Pt-2** and **Pt-3** are close to that at RT (1–2 ns), therefore the fluorescence feature of the luminescence of these complexes is proved unambiguously. For **Pt-0** and **Pt-4**, the luminescence intensity at 77 K generally increased compared to that at RT. The lifetime of the emission at the higher energy side of the dual emission bands is a few ns, thus these emission bands can be assigned as fluorescence. For the emission at a lower energy region, the luminescence lifetime increased by *ca.* 2-fold at 77 K. The lifetimes of 424.4 μ s and 623.3 μ s were observed for **Pt-0** and **Pt-4**, respectively.

Nanosecond time-resolved transient difference absorption spectroscopy

In order to study the triplet excited states of the complexes, the nanosecond time-resolved transient difference absorption

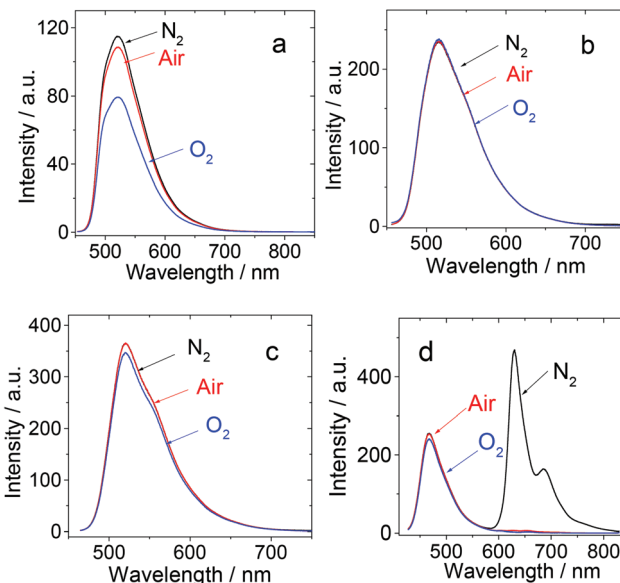


Fig. 2 The emission spectra of the Pt(II) complexes under different atmospheres. (a) **Pt-1** ($\lambda_{\text{ex}} = 449$ nm), (b) **Pt-2** ($\lambda_{\text{ex}} = 448$ nm), (c) **Pt-3** ($\lambda_{\text{ex}} = 459$ nm), (d) **Pt-4** ($\lambda_{\text{ex}} = 420$ nm). In toluene, $c = 1.0 \times 10^{-5}$ M, 25 °C.

spectra of the complexes were studied (Fig. 4).⁴⁵ Upon pulsed laser excitation, bleaching bands at the steady state UV-Vis absorption band were observed. Moreover, similar transient absorption features in the range 500–700 nm were observed. Since **Pt-1**, **Pt-2** and **Pt-3** show similar positive transient absorption bands and lifetimes, we propose that the triplet excited state is localized on the coumarin unit. As a support for this postulation, **Pt-4** and **Pt-0** show drastically different transient absorption features, *e.g.* their triplet state lifetimes are much longer.

In order to study the efficiency of the triplet excited state production of the complexes, the photosensitization of singlet oxygen ($^1\text{O}_2$) with the complexes upon photoexcitation was

Table 1 Photophysical parameters of **Pt-0–Pt-5**, **L-1** and **L-2**

	λ_{abs}^a	ϵ^b	λ_{em}^c	Φ_{F}^d	Φ_{P}^e	τ_{F}^f (ns)		τ_{P}^g (μ s)		τ_{T}^h / μ s	Φ_{Δ}^i
						298 K	77 K	298 K	77 K		
Pt-0	421	2.09	458/628	13.4%	1.05%	0.5	1.2	232.7	424.4	139.9	0.86
Pt-1	449	3.37	521	66.4%	—	2.8	2.8	—	—	16.0	0.21
Pt-2	448	4.81	514	0.95%	—	1.5	1.1	—	—	20.3	0.99
Pt-3	459	7.68	520	3.8%	—	1.1	1.3	—	—	17.2	0.86
Pt-4	426	2.39	469/630	1.1%	2.4%	1.0	1.0	278.6	623.3	100.7	0.82
Pt-5^j	323	2.45	—	—	—	—	—	—	—	—	0.07
L-1	436	1.91	456	81.9%	—	2.4	—	—	—	—	0.12
L-2	350	1.78	401	—	—	0.2	—	—	—	—	—

^a In toluene (1.0×10^{-5} M). ^b Molar extinction coefficient at the absorption maxima ϵ : $10^4 \text{ cm}^{-1} \text{ M}^{-1}$. ^c In toluene. ^d In toluene, with quinine sulfate ($\Phi = 0.546$ in 0.5 M H_2SO_4) as the standards. ^e In toluene, with $[\text{Ru}(\text{dmb})_3(\text{PF}_6)_2]$ ($\Phi = 0.073$ in acetonitrile) as the standards. ^f Luminescence lifetime, $\lambda_{\text{ex}} = 443$ nm, at RT (**Pt-0–Pt-4** in deaerated ethanol–methanol, 4 : 1, v/v; **L-1** and **L-2** in deaerated toluene) and 77 K (in ethanol–methanol, 4 : 1, v/v). ^g Phosphorescence lifetime, **Pt-0** ($\lambda_{\text{ex}} = 420$ nm), **Pt-4** ($\lambda_{\text{ex}} = 420$ nm), at RT (in deaerated ethanol–methanol, 4 : 1, v/v) and 77 K (in ethanol–methanol, 4 : 1, v/v). ^h Triplet state lifetime, determined with nanosecond time-resolved transient difference absorption spectroscopy, $\lambda_{\text{ex}} = 355$ nm, $c = 1.0 \times 10^{-5}$ M in aerated and deaerated toluene. ⁱ Quantum yield of singlet oxygen ($^1\text{O}_2$), **Pt-0–Pt-4** with TPP as standard ($\Phi_{\Delta} = 0.62$ in CH_2Cl_2), **Pt-5** with Rose Bengal as standard ($\Phi_{\Delta} = 0.8$ in methanol), $c = 1.0 \times 10^{-5}$ M in CH_2Cl_2 and methanol. ^j **Pt-5** is non-luminescent, therefore some photophysical parameters were not measured.

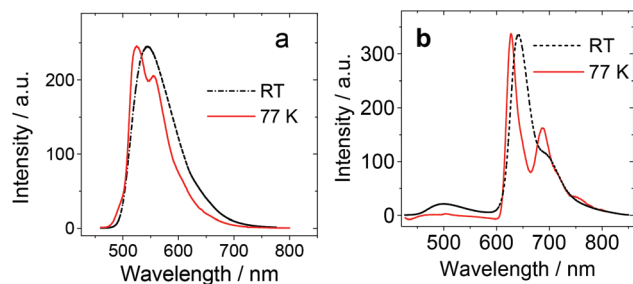


Fig. 3 Photoluminescence spectra of the complexes at RT and 77 K. (a) **Pt-1** ($\lambda_{\text{ex}} = 449$ nm) and (b) **Pt-4** ($\lambda_{\text{ex}} = 420$ nm). $c = 6.0 \times 10^{-5}$ M in $\text{C}_2\text{H}_5\text{OH}-\text{CH}_3\text{OH}$ (4 : 1, v/v).

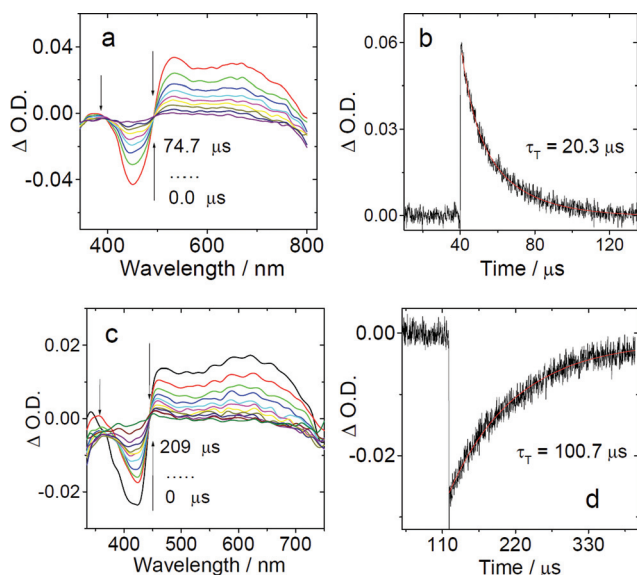


Fig. 4 Nanosecond time-resolved transient difference absorption spectra of (a) **Pt-2** and (c) **Pt-4** after pulsed excitation ($\lambda_{\text{ex}} = 355$ nm). Decay traces of (b) **Pt-2** at 530 nm and (d) **Pt-4** at 430 nm. $c = 1.0 \times 10^{-5}$ M in deaerated toluene, 25 $^\circ\text{C}$.

studied and the $^1\text{O}_2$ quantum yields (Φ_Δ) were determined (Table 1 and ESI †). The Φ_Δ values of **Pt-2**, **Pt-3** and **Pt-4** are large (0.82–0.99). For **Pt-1** and **Pt-5**, however, it is much smaller (0.21 and 0.07).

DFT calculations on the complexes: spin density surfaces and electronic transitions

In order to study the triplet states of the complexes, the spin density surfaces were calculated using DFT methods. Generally the triplet excited states are localized on the organic ligands, instead of the Pt(II) coordination centers (Fig. 5). This result is in agreement with the long-lived triplet excited states of the complexes.

The ground state geometries of the complexes were optimized using DFT methods. For **Pt-1**, the dihedral angle between the coumarin and the thienyl part is 1.89 degree, indicating a good π -conjugation. The two arylacetylides take a non-coplanar geometry (see ESI † for details). The UV-vis absorption

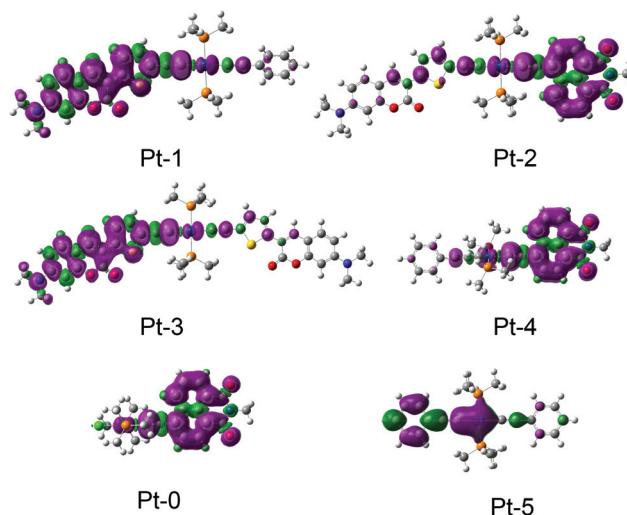


Fig. 5 Spin density of the complexes **Pt-0**, **Pt-1**, **Pt-2**, **Pt-3**, **Pt-4** and **Pt-5**. Calculated based on the optimized triplet state by DFT at the B3LYP/6-31G(d)/LanL2DZ level using Gaussian 09W.

of **Pt-1** was calculated based on the optimized ground state geometry.

The absorption band in the visible region was predicted at 491 nm, which is close to the experimental result of 449 nm (Fig. 1). It is known that the DFT methods usually underestimate the excitation energy for charge transfer. The electronic components of the transition are H \rightarrow L, which can be assigned as the IL and MLCT mixed transition, with IL as the major contributor. The singlet–triplet state energy gaps were also calculated (see ESI † for details). The energy level of the T_1 state was estimated to be 1.65 eV (735 nm). H \rightarrow L is involved in the T_1 state, thus the T_1 state can be assigned as the ^3IL state, which is in agreement with the spin density analysis and the long-lived triplet excited state observed for **Pt-1**.

The geometry of **Pt-3** was also optimized. The calculated absorption is close to the experimental observations. The energy gap of S_1/T_1 was calculated as 774 nm (see ESI † for details). T_1 state is with a significant intraligand state feature.

Ratiometric O_2 sensing

Since **Pt-4** shows fluorescence–phosphorescence dual emission, fluorescence is insensitive to O_2 , but the phosphorescence is highly sensitive to O_2 , thus **Pt-4** was used for ratiometric luminescent O_2 sensing.^{22,44,46} Luminescent O_2 sensing is important for chemical, biological and environmental science. Ratiometric O_2 sensing is more favorable under some circumstances than O_2 sensing based on luminescence intensity.^{46–49} However, reports on ratiometric O_2 sensing with *uni-chromophore* complexes are rare.^{22,46} Usually two methods were used for ratiometric O_2 sensing. One is to use two luminophores, for which one is fluorescent, and another is phosphorescent. But the different photostability may make the sensor less durable. The second method is to use a luminophore with fluorescence–phosphorescence dual emission.^{22,42,44,46} However, it is still a substantial challenge to

develop such fluorescence–phosphorescence dual emissive luminophores.

Previously Pt(II) and Ir(III) complexes have been reported to show the fluorescence–phosphorescence dual emission, but the ratiometric O₂ sensitivity was not studied.⁴² Recently we studied the ratiometric O₂ sensing with cyclometalated Pt(II) complexes.⁴⁴ It is clear that the diversity of such luminophores needs to be increased.⁴⁶ **Pt-4** shows the dual emission, thus the ratiometric O₂ sensing using **Pt-4** was studied (Fig. 6).

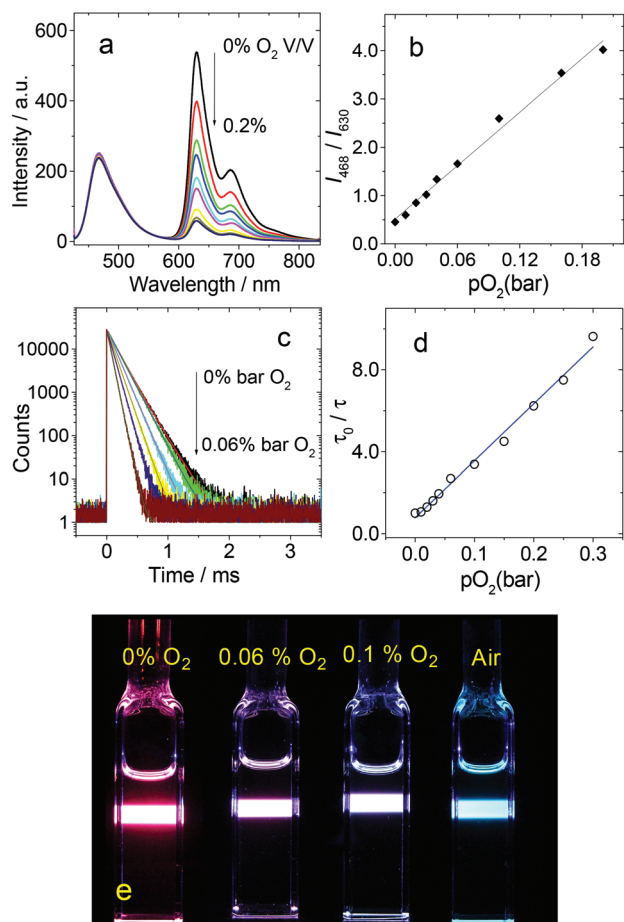


Fig. 6 Ratiometric luminescence response of **Pt-4** to variation of the O₂ concentration. (a) Emission spectra of **Pt-4** in the presence of 0%, 0.01%, 0.03%, 0.04%, 0.06%, 0.1%, 0.16%, 0.2% O₂. (b) The linear correlation between the ratiometric photoluminescence response toward the O₂ partial pressure. (c) Phosphorescence lifetime ($\lambda_{\text{ex}} = 420 \text{ nm}$) variation of **Pt-4** in the presence of 0%, 0.01%, 0.02%, 0.03%, 0.04%, 0.06%, 0.1%, 0.15%, 0.2% O₂. (d) The linear correlation between the phosphorescence lifetime ratios τ_0/τ toward the O₂ partial pressure. (e) Emission images of **Pt-4** under different O₂ partial pressure. c [**Pt-4**] = $1.0 \times 10^{-5} \text{ M}$ in toluene, 25 °C.

With increasing O₂ partial pressure, the phosphorescence at 630 nm was drastically quenched, but the fluorescence at 469 nm was intact. Thus ratiometric O₂ sensing using emission intensity can be established (Fig. 6a and 6b). Furthermore, the phosphorescence lifetimes were monitored with increasing O₂ partial pressure (Fig. 6c and 6d). The O₂ sensing was also monitored with lifetime changes (Fig. 6 and Table 2). With increasing O₂ partial pressure, the fluorescence lifetime hardly changed (Table 2, the fluctuations of the lifetime values are within experimental errors), but the phosphorescence lifetime decreased sharply from 169.4 μs to 27.2 μs .

The balanced fluorescence–phosphorescence emission is beneficial for ratiometric O₂ sensing. To the best of our knowledge, ratiometric O₂ sensing based on uni-chromophore sensing material is rarely reported.

Triplet–triplet annihilation upconversion

TTA upconversion has attracted much attention, due to its potential applications in photovoltaics,^{9–11,50–52} photocatalysis,⁵³ luminescent bioimaging,⁵⁴ and O₂ sensing.⁵⁵ Triplet photosensitizers are crucial for TTA upconversion.^{9–11} Conventionally the triplet photosensitizers are limited to the Pt(II) or Pd(II) porphyrin complexes.^{9,10} However, the absorption wavelength and the T₁ excited state energy levels of these complexes cannot be readily optimized. Ru(II) and Ir(III) complexes and some organic compounds were used as triplet photosensitizers for TTA upconversion.^{56,57} However, these compounds usually show weak absorption of visible light and short-lived triplet excited states. Recently we developed a series of Ru(II), Pt(II), Ir(III) and Re(I) complexes as triplet photosensitizers for TTA upconversion.^{10,58–65} These complexes show strong absorption in the visible region and long-lived triplet excited states.

However, to the best of our knowledge, very few linear bis(alkylphosphine) Pt(II) bisacetylides complexes have been used as triplet photosensitizers for TTA upconversion.^{10,21c} Herein the Pt(II) complexes were used for TTA upconversion.

A triplet acceptor is an essential component for TTA upconversion.^{9–11} One of the prerequisites for a useful triplet photosensitizer is that the energy level of the T₁ state of a triplet acceptor must be lower than the energy level of the T₁ state of the photosensitizer. **Pt-1–Pt-3** are not phosphorescent and the triplet excited state energy level cannot be accessed easily, therefore, 9,10-diphenylanthracene (DPA) was used as the triplet acceptor for the preliminary tests. The T₁ state energy level of DPA is 1.77 eV, which is lower than the T₁ state energy level of **Pt-4** (approximated as 1.97 eV based on the RT phosphorescence at 630 nm). The complexes show their

Table 2 The variation of the luminescence lifetime of **Pt-4** against the O₂ concentrations (v/v% in O₂–N₂ mixture)^a

[O ₂] ^b	0.0	0.01	0.02	0.03	0.04	0.06	0.1	0.15	0.2
$\tau_{468} \text{ (ns)}^c$	0.34	0.40	0.46	0.41	0.46	0.48	0.55	0.55	0.65
$\tau_{630} \text{ (}\mu\text{s)}^d$	169.4	160.0	130.6	105.7	87.0	62.9	50.2	37.7	27.2

^a c [**Pt-4**] = $1.0 \times 10^{-5} \text{ M}$ in toluene, 25 °C. ^b O₂ concentrations, v/v $\times 100$. ^c Luminescence lifetime, excited with pulsed laser ($\lambda_{\text{ex}} = 405 \text{ nm}$), 298 K (in deaerated toluene). ^d Phosphorescence lifetime, excited with pulsed laser ($\lambda_{\text{ex}} = 420 \text{ nm}$), 298 K (in deaerated toluene).

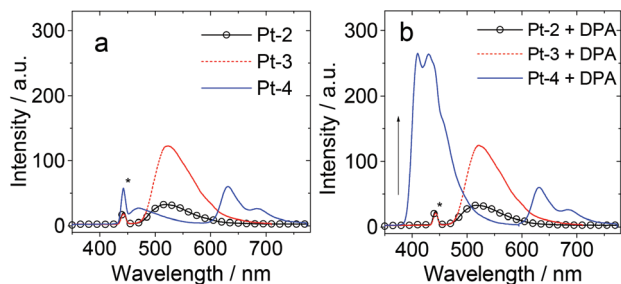


Fig. 7 Emission and upconversion of the complexes with 445 nm (5 mW) laser excitation. (a) Emission of the complexes alone. (b) The up-converted DPA fluorescence and the residual fluorescence and phosphorescence of the complexes. (c) [DPA] = 6.0×10^{-5} M; [sensitizers] = 1.0×10^{-5} M in deaerated toluene. The asterisks in (a) and (b) indicate the scattered 445 nm excitation laser (5 mW), 25 °C.

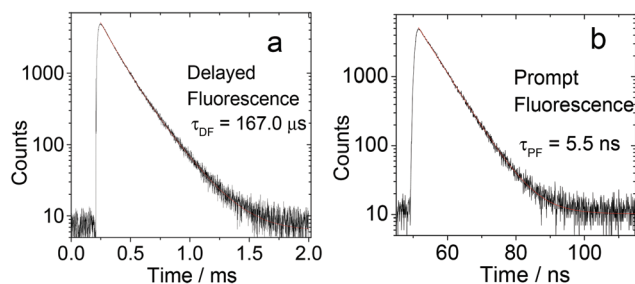


Fig. 8 Delayed fluorescence observed in the TTA upconversion with (a) **Pt-4** as the triplet photosensitizer and DPA as the triplet acceptor. Excited at 445 nm and monitored at 410 nm. (b) The prompt fluorescence decay of DPA determined in a different experiment (excited with picosecond 405 nm laser, the decay of the emission was monitored at 410 nm). (c) [DPA] = 6.0×10^{-5} M; [sensitizers] = 1.0×10^{-5} M in deaerated toluene, 25 °C.

characteristic emission upon 445 nm laser excitation. For example, **Pt-4** shows fluorescence–phosphorescence dual emission, whereas complexes **Pt-2** and **Pt-3** show only the fluorescence. Blue emission was observed for **Pt-4** upon the addition of DPA to the solution, but no blue emission was observed for **Pt-2** and **Pt-3** (Fig. 7b). **Pt-5** cannot be photo-excited at 445 nm.

In order to unambiguously confirm that the blue emission is due to the upconverted emission of DPA, the luminescence lifetime of the blue emission band in Fig. 7b was measured (Fig. 8).^{66–68} An exceptionally long-lived lifetime of 167.0 μ s was observed. This delayed luminescence lifetime is a typical feature of the TTA upconversion. In comparison, the prompt fluorescence lifetime of DPA was determined as 5.5 ns (Fig. 8b).

The upconversion is clearly visible to the eyes (Fig. 9). For **Pt-2** and **Pt-3**, green emission was observed, which is due to the residual fluorescence of the photosensitizers. For **Pt-4**, a purple emission was observed, which is due to the simultaneous blue/red emission. In the presence of the triplet photosensitizer DPA, a blue emission band was observed for **Pt-4**, but the emission wavelength of the **Pt-2** and **Pt-3** solutions did not change, in agreement with the lack of TTA

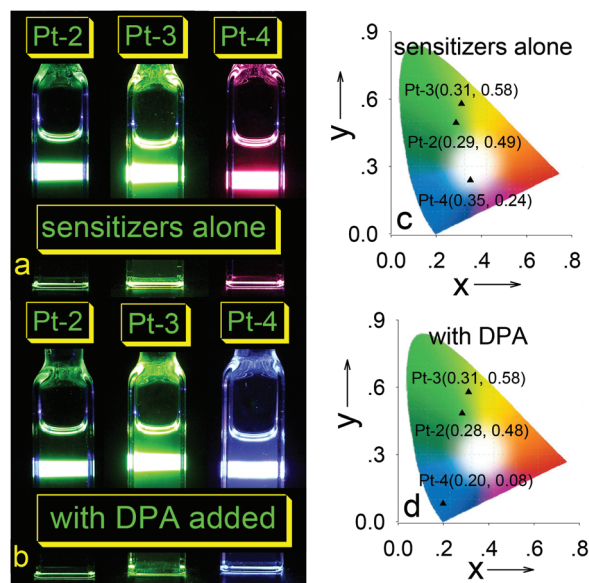


Fig. 9 (a) Photographs of the emission of sensitizers alone and (b) the upconversion. (c) CIE diagram of the emission of sensitizers alone and (d) in the presence of DPA (upconversion). λ_{ex} = 445 nm (laser power: 5 mW). In deaerated toluene, [sensitizer] = 1.0×10^{-5} M, [DPA] = 6.0×10^{-5} M, 25 °C.

upconversion for **Pt-2** and **Pt-3** (with triplet acceptor DPA, Fig. 9).

In order to study the efficiency of the triplet–triplet-energy-transfer (TTET) process, which is crucial for the TTA upconversion, the triplet state quenching of the triplet photosensitizer was measured using nanosecond transient absorption (see ESI† for details). Significant quenching was observed for **Pt-4**, with quenching constants of $5.38 \times 10^4 \text{ M}^{-1}$ (Table 3). For **Pt-2** and **Pt-3**, however, the quenching of the triplet state lifetime is not significant, which may be responsible for the lack of TTA upconversion for **Pt-2** and **Pt-3**.

Pt-2 and **Pt-3** show high singlet O_2 sensitizing quantum yields (Table 1), but no upconversion was observed for these complexes with DPA as the triplet acceptor. DFT calculations indicated that the T_1 state energy levels of these complexes are lower than that of **Pt-4** (see ESI† for details). It is known that for TTA upconversion, the T_1 state energy level of the triplet

Table 3 Triplet excited state lifetimes (τ), Stern–Volmer quenching constant (K_{SV}) and bimolecular quenching constants (k_q) of the Pt(II) sensitizers. In deaerated toluene solution, 20 °C

	$\tau_T / \mu\text{s}$	$K_{\text{SV}} / 10^3 \text{ M}^{-1}$		$k_q / 10^9 \text{ M}^{-1} \text{ s}^{-1}$		Φ_{UC}^a	
		Py	DPA	Py	DPA	Py	DPA
Pt-0	139.9	1.0	196.0	0.007	1.40	— ^b	— ^b
Pt-1	16.0	8.4	0.17	0.53	0.01	— ^b	— ^b
Pt-2	20.3	42.8	0.80	2.11	0.039	17.1%	— ^b
Pt-3	17.2	93.5	1.3	5.44	0.076	13.6%	— ^b
Pt-4	100.7	9.5	537.8	0.09	5.34	— ^b	27.2%

^a Upconversion quantum yields, **Pt-4** with coumarin-6 as the standard ($\Phi_{\text{F}} = 78\%$ in ethanol), **Pt-2** and **Pt-3** with diiodo-BODIPY ($\Phi_{\text{F}} = 2.7\%$ in acetonitrile) as the standard. ^b No results were obtained.

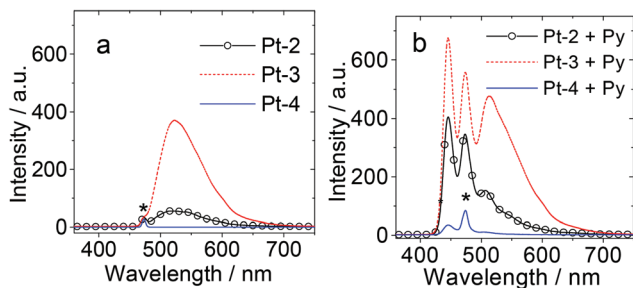


Fig. 10 Emission and upconversion of the complexes with 473 nm (5 mW) laser excitation. (a) Emission of the complexes alone. (b) The upconverted perylene (Py) fluorescence and the residual fluorescence of the triplet photosensitizers. c [Py] = 4.0×10^{-5} M; c [sensitizers] = 1.0×10^{-5} M in deaerated toluene. The asterisks in (a) and (b) indicate the scattered 473 nm excitation laser (5 mW), 25 °C.

acceptor must be lower than that of the triplet photosensitizer. Therefore, we studied the TTA upconversion with a different triplet acceptor that shows a lower T_1 state energy level, *i.e.* perylene ($E_{T1} = 1.53$ eV).

With perylene as the triplet photosensitizer, TTA upconversion was observed for **Pt-2** and **Pt-3** (Fig. 10). **Pt-4** was not studied under these conditions because this complex cannot be excited by the 473 nm laser.

The delayed fluorescence lifetimes of the TTA upconversion for **Pt-2** and **Pt-3** with perylene as the triplet acceptor were also studied (see ESI† for details). The long-lived luminescence lifetimes are in agreement with the TTA upconversion feature.

The upconversion with perylene as the triplet acceptor is also visible to eyes (see ESI† for details). For **Pt-2** and **Pt-3** alone, the emission color is green upon 473 nm laser excitation. In the presence of perylene, the emission colour of the solution turns blue. For **Pt-4**, however, no upconversion was observed because **Pt-4** cannot be photoexcited at 473 nm, due to its absorption in this blue-shifted region.

The TTET with perylene as the triplet acceptor were also studied with the triplet state lifetime quenching experiments (Fig. 11). **Pt-2** and **Pt-3** give much larger quenching constants than the other complexes. The photophysical properties related to the upconversion are summarized in Table 3.

Time-resolved emission spectroscopy

The emission of **Pt-4** alone and the emission of TTA upconversion with **Pt-4** as triplet photosensitizers were studied by using nanosecond and microsecond time-resolved emission spectra (TRES, Fig. 12). For **Pt-4** alone, the TRES of the phosphorescence and the fluorescence bands were recorded separately (note that there is substantial difference between the lifetimes of the two emission bands, it is technically difficult to record the two emission bands simultaneously with one pulsed laser). The results confirmed that the phosphorescence decay gives much longer lifetime (Fig. 12a, 201.2 μ s) than the fluorescence band (Fig. 12b, 0.5 ns). The difference between the lifetime values and that determined in the previous section

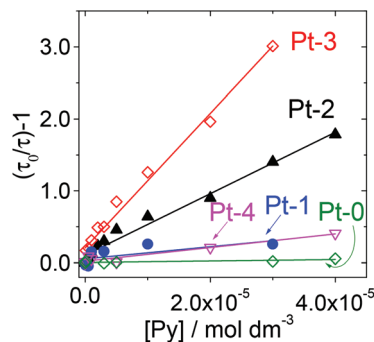


Fig. 11 Stern–Volmer plots for lifetime quenching of **Pt-0**, **Pt-1**, **Pt-2**, **Pt-3** and **Pt-4** with increasing the concentration of perylene (Py) after pulsed excitation ($\lambda_{ex} = 355$ nm). c [sensitizers] = 1.0×10^{-5} M in deaerated toluene, 25 °C.

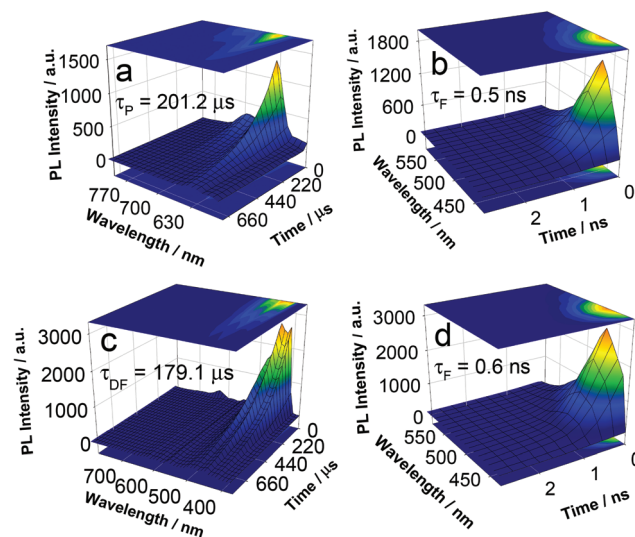
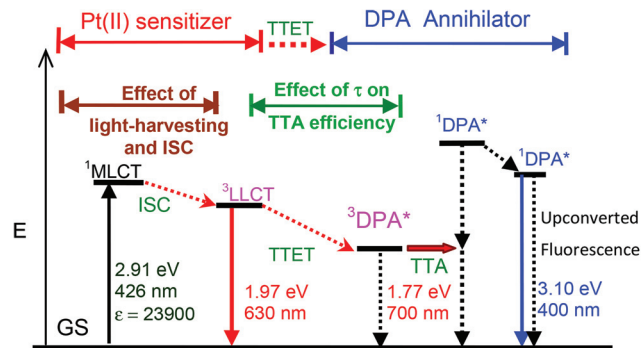


Fig. 12 Time-resolved emission spectra (TRES) of **Pt-4** alone and the TTA upconversion with the DPA as the triplet acceptor. **Pt-4** alone: (a) the phosphorescence region was measured (570 nm–800 nm, $\tau = 201.2$ μ s) excited with nanosecond pulsed laser (445 nm) and (b) the fluorescence region was measured (430 nm–570 nm, $\tau = 0.5$ ns) excited with picosecond pulsed laser (443 nm). TRES of **Pt-4** in the presence of DPA: (c) upconverted emission in the range of 400 nm–500 nm was observed ($\tau = 179.1$ μ s) with nanosecond pulsed laser (445 nm) and (d) fluorescence range 430 nm–520 nm was observed ($\tau = 0.6$ ns) excited with pico-second pulsed laser (443 nm). c [DPA] = 6.0×10^{-5} M; c [photosensitizers] = 1.0×10^{-5} M in deaerated toluene, 25 °C.

(Table 1) is due to the fact that the background dynamics of the pulsed laser cannot be calibrated in the TRES mode.

The TRES of **Pt-4** in the presence of DPA (TTA upconversion) was also studied (Fig. 12c and d). In the presence of DPA, the fluorescence band shows no changes (Fig. 12d, 0.6 ns). A long-lived emission band in the 400–500 nm region was observed (Fig. 12c, $\tau = 179.1$ μ s), which is due to the upconverted emission. The fluorescence emission band in the region of 430 nm–520 nm was also measured (Fig. 12d), the decay of the fluorescence band did not change compared to that of **Pt-4** alone (lifetime = 0.5 ns). This is a reasonable result since the singlet excited state of the triplet photosensitizer is not involved in the TTET process, therefore the singlet excited



Scheme 2 Jablonski diagram of triplet-triplet-annihilation (TTA) upconversion with **Pt-4** as a triplet sensitizer (the triplet states of sensitizers are emissive) and 9,10-diphenylanthracene (DPA) was the triplet acceptor. TTET stands for triplet-triplet-energy-transfer.

state of the photosensitizer will not be alternated. These results confirmed the triplet-triplet annihilation upconversion. Similar TRES spectra were observed for **Pt-2** (see ESI† for details).

The TTA upconversion process can be summarized in Scheme 2. The light-harvesting ability and the lifetimes of the triplet excited states of the triplet photosensitizers are crucial for the TTA upconversion. The TTET process can be enhanced with the long-lived triplet excited states of the triplet photosensitizer.

Conclusions

In conclusion, a series of symmetric and unsymmetric *trans*-bis(alkylphosphine) Pt(II) bisacetylides were prepared, and their photophysical properties were studied with steady state and time-resolved spectroscopies, as well as DFT calculations. Thienyl coumarin and naphthalimide acetylides were used as ligands. To the best of our knowledge, this is the first time that coumarin and naphthalimide acetylides have been used for the preparation of *trans*-bis(alkylphosphine) Pt(II) bis(acetylides) complexes. These complexes show *strong absorption of visible light* and *long-lived triplet excited states* (16.0–139.9 μs), which are drastically different from the conventional *trans*-bisphosphine Pt(II) bis(acetylides) complexes. The complexes with naphthalimide and phenyl acetylides show *room temperature fluorescence-phosphorescence dual emission*, whereas the other complexes showed only fluorescence emission. Long-lived triplet excited states were observed. The complexes were used as triplet photosensitizers for ratiometric O₂ sensing and triplet-triplet annihilation upconversion and upconversion quantum yields up to 27.2% were observed. Our results are useful for preparation of bis(alkylphosphine) Pt(II) bisacetylides complexes that show strong absorption of visible light and long-lived triplet excited states, and for the application of these complexes in photocatalysis, photovoltaics and triplet-triplet annihilation upconversion.

Acknowledgements

We thank the NSFC (20972024, 21073028 and 21273028), the Science Foundation Ireland (SFI E.T.S. Walton Program 11/W.1/E2061), the Royal Society (UK) and NSFC (China-UK Cost-Share Science Networks, 21011130154), the Fundamental Research Funds for the Central Universities (DUT10ZD212), Ministry of Education (NCET-08-0077 and SRFDP-20120041130005) for financial support.

Notes and references

- 1 K. Mori, K. Watanabe, K. Fuku and H. Yamashita, *Chem.-Eur. J.*, 2012, **18**, 415–418.
- 2 W.-G. Wang, F. Wang, H.-Y. Wang, C.-H. Tung and L.-Z. Wu, *Dalton Trans.*, 2012, **41**, 2420–2426.
- 3 F.-R. Dai, H.-M. Zhan, Q. Liu, Y.-Y. Fu, J.-H. Li, Q.-W. Wang, Z. Xie, L. Wang, F. Yan and W.-Y. Wong, *Chem.-Eur. J.*, 2012, **18**, 1502–1511.
- 4 G. Zhou, W.-Y. Wong, S.-Y. Poon, C. Ye and Z. Lin, *Adv. Funct. Mater.*, 2009, **19**, 531–544.
- 5 S.-C. Chan, M. C. W. Chan, Y. Wang, C.-M. Che, K.-K. Cheung and N. Zhu, *Chem.-Eur. J.*, 2001, **7**, 4180–4190.
- 6 C. K. M. Chan, C.-H. Tao, K.-F. Li, K. M.-C. Wong, N. Zhu, K.-W. Cheah and V. W.-W. Yam, *Dalton Trans.*, 2011, **40**, 10670–10685.
- 7 (a) R. Liu, A. Azenkeng, Y. Li and W. Sun, *Dalton Trans.*, 2012, **41**, 12353–12357; (b) P. Shao, Y. Li, J. Yi, T. M. Pritchett and W. Sun, *Inorg. Chem.*, 2010, **49**, 4507–4517.
- 8 (a) Y. Sun and S. Wang, *Inorg. Chem.*, 2009, **48**, 3755–3767; (b) V. F. Moreira, F. L. T. Greenwood and M. P. Coogan, *Chem. Commun.*, 2010, **46**, 186–202; (c) Q. Zhao, F. Li and C. Huang, *Chem. Soc. Rev.*, 2010, **39**, 3007–3030; (d) Y. Tang, H.-R. Yang, H.-B. Sun, S.-J. Liu, J.-X. Wang, Q. Zhao, X.-M. Liu, W.-J. Xu, S.-B. Li and W. Huang, *Chem.-Eur. J.*, 2013, **19**, 1311–1319; (e) E. Baggaley, J. A. Weinstein and J. A. G. Williams, *Coord. Chem. Rev.*, 2012, **256**, 1762–1785; (f) P.-H. Lanoë, J.-L. Fillaut, L. Toupet, J. A. Gareth Williams, H. Le Bozec and V. Guerschais, *Chem. Commun.*, 2008, 4333–4335.
- 9 T. N. Rachford and F. N. Castellano, *Coord. Chem. Rev.*, 2010, **254**, 2560–2573.
- 10 J. Zhao, S. Ji and H. Guo, *RSC Adv.*, 2011, **1**, 937–950.
- 11 (a) P. Ceroni, *Chem.-Eur. J.*, 2011, **17**, 9560–9564; (b) A. Monguzzi, R. Tubino, S. Hoseinkhani, M. Campione and F. Meinardi, *Phys. Chem. Chem. Phys.*, 2012, **14**, 4322–4332; (c) G. Bergamini, P. Ceroni, M. Maestri, V. Balzani, S.-K. Lee and F. Vögtle, *Photochem. Photobiol. Sci.*, 2004, **3**, 898–905.
- 12 (a) P. Du and R. Eisenberg, *Chem. Sci.*, 2010, **1**, 502–506; (b) T. J. Wadas, R. J. Lachicotte and R. Eisenberg, *Inorg. Chem.*, 2003, **42**, 3772–3778.

- 13 (a) Y. Liu, S. Jiang, K. Glusac, D. H. Powell, D. F. Anderson and K. S. Schanze, *J. Am. Chem. Soc.*, 2002, **124**, 12412–12413; (b) K.-Y. Kim, S. Liu, M. E. Köse and K. S. Schanze, *Inorg. Chem.*, 2006, **45**, 2509–2519.
- 14 (a) C. K. M. Chan, C.-H. Tao, H.-L. Tam, N. Zhu, V. W.-W. Yam and K.-W. Cheah, *Inorg. Chem.*, 2009, **48**, 2855–2864; (b) D. Nolan, B. Gil, F. A. Murphy and S. M. Draper, *Eur. J. Inorg. Chem.*, 2011, **21**, 3248–3256.
- 15 I. Eryazici, C. N. Moorefield and G. R. Newkome, *Chem. Rev.*, 2008, **108**, 1834–1895.
- 16 J. A. G. Williams, *Top. Curr. Chem.*, 2007, **281**, 205–268.
- 17 (a) C. E. Whittle, J. A. Weinstein, M. W. George and K. S. Schanze, *Inorg. Chem.*, 2001, **40**, 4053–4062; (b) B. Ma, P. I. Djurovich and M. E. Thompson, *Coord. Chem. Rev.*, 2005, **249**, 1501–1510.
- 18 (a) I. Stengel, C. A. Strassert, E. A. Plummer, C.-H. Chien, L. D. Cola and P. Bäuerle, *Eur. J. Inorg. Chem.*, 2012, **11**, 1795–1809; (b) M. Lindgren, B. Minaev, E. Glimsdal, R. Vestberg, R. Westlund and E. Malmström, *J. Lumin.*, 2007, **124**, 302–310; (c) B. Minaev, H. Ågren and F. De Angelis, *Chem. Phys.*, 2009, **358**, 245–257; (d) S. Fantacci and F. De Angelis, *Coord. Chem. Rev.*, 2011, **358**, 2704–2726; (e) J. Zhao, W. Wu, J. Sun and S. Guo, *Chem. Soc. Rev.*, 2013, DOI: 10.1039/c3cs35531d.
- 19 W.-Y. Wong and C.-L. Ho, *Coord. Chem. Rev.*, 2006, **250**, 2627–2690.
- 20 W.-Y. Wong and P. D. Harvey, *Macromol. Rapid Commun.*, 2010, **31**, 671–713.
- 21 (a) K. Glusac, M. E. Ko1se, H. Jiang and K. S. Schanze, *J. Phys. Chem. B*, 2007, **111**, 929–940; (b) T. M. Cooper, D. M. Krein, A. R. Burke, D. G. McLean, J. E. Haley, J. Slagle, J. Monahan and A. Fratini, *J. Phys. Chem. A*, 2012, **116**, 139–149; (c) W. Wu, J. Zhao, J. Sun, L. Huang and X. Yi, *J. Mater. Chem. C*, 2013, **1**, 705–716.
- 22 H. Hochreiner, I. S. Barraquán, J. M. C. Fernández and A. S. Medel, *Talanta*, 2005, **66**, 611–618.
- 23 L. Ma, H. Guo, Q. Li, S. Guo and J. Zhao, *Dalton Trans.*, 2012, **41**, 10680–10689.
- 24 X. Yi, P. Yang, D. Huang and J. Zhao, *Dyes Pigm.*, 2013, **96**, 104–115.
- 25 D. Huang, J. Zhao, W. Wu, X. Yi, P. Yang and J. Ma, *Asian J. Org. Chem.*, 2012, **1**, 264–273.
- 26 S. Guo, J. Sun, L. Ma, W. You, P. Yang and J. Zhao, *Dyes Pigm.*, 2013, **96**, 449–458.
- 27 M. J. Frisch, G. W. Trucks, H. B. Schlegel, G. E. Scuseria, M. A. Robb, J. R. Cheeseman, G. Scalmani, V. Barone, B. Mennucci, G. A. Petersson, H. Nakatsuji, M. Caricato, X. Li, H. P. Hratchian, A. F. Izmaylov, J. Bloino, G. Zheng, J. L. Sonnenberg, M. Hada, M. Ehara, K. Toyota, R. Fukuda, J. Hasegawa, M. Ishida, T. Nakajima, Y. Honda, O. Kitao, H. Nakai, T. Vreven, J. A. Montgomery Jr., J. E. Peralta, F. Ogliaro, M. Bearpark, J. J. Heyd, E. Brothers, K. N. Kudin, V. N. Staroverov, R. Kobayashi, J. Normand, K. Raghavachari, A. Rendell, J. C. Burant, S. S. Iyengar, J. Tomasi, M. Cossi, N. Rega, J. M. Millam, M. Klene, J. E. Knox, J. B. Cross, V. Bakken, C. Adamo, J. Jaramillo, R. Gomperts, R. E. Stratmann, O. Yazyev, A. J. Austin, R. Cammi, C. Pomelli, J. W. Ochterski, R. L. Martin, K. Morokuma, V. G. Zakrzewski, G. A. Voth, P. Salvador, J. J. Dannenberg, S. Dapprich, A. D. Daniels, Ö. Farkas, J. B. Foresman, J. V. Ortiz, J. Cioslowski and D. J. Fox, *Gaussian 09W(Revision A.1)*, Gaussian Inc., Wallingford CT, 2009.
- 28 H. Sun, H. Guo, W. Wu, X. Liu and J. Zhao, *Dalton Trans.*, 2011, **40**, 7834–7841.
- 29 Z. Ning and H. Tian, *Chem. Commun.*, 2009, 5483–5495.
- 30 Y. Chen, J. Zhao, L. Xie, H. Guo and Q. Li, *RSC Adv.*, 2012, **2**, 3942–3953.
- 31 H. Guo, M. L. M. Small, S. Ji, J. Zhao and F. N. Castellano, *Inorg. Chem.*, 2010, **49**, 6802–6804.
- 32 H. Guo, S. Ji, W. Wu, W. Wu, J. Shao and J. Zhao, *Analyst*, 2010, **135**, 2832–2840.
- 33 S. Ji, W. Wu, J. Zhao, H. Guo and W. Wu, *Eur. J. Inorg. Chem.*, 2012, **19**, 3183–3190.
- 34 W.-S. Tang, X.-X. Lu, K. M.-C. Wong and V. W.-W. Yam, *J. Mater. Chem.*, 2005, **15**, 2714–2720.
- 35 S. C. F. Kui, F.-F. Hung, S.-L. Lai, M.-Y. Yuen, C.-C. Kwok, K.-H. Low, S. S.-Y. Chui and C.-M. Che, *Chem.–Eur. J.*, 2012, **18**, 96–109.
- 36 S.-C. Chan, M. C. W. Chan, Y. Wang, C.-M. Che, K.-K. Cheung and N. Zhu, *Chem.–Eur. J.*, 2001, **7**, 4180–4190.
- 37 Y. Chi and P.-T. Chou, *Chem. Soc. Rev.*, 2010, **39**, 638–655.
- 38 S. Goeb, A. A. Rachford and F. N. Castellano, *Chem. Commun.*, 2008, 814–816.
- 39 C. J. Adams, N. Fey, Z. A. Harrison, I. V. Sazanovich, M. Towrie and J. A. Weinstein, *Inorg. Chem.*, 2008, **47**, 8242–8257.
- 40 M. Hissler, W. B. Connick, D. K. Geiger, J. E. McGarrah, D. Lipa, R. J. Lachicotte and R. Eisenberg, *Inorg. Chem.*, 2000, **39**, 447–457.
- 41 C. E. Whittle, J. A. Weinstein, M. W. George and K. S. Schanze, *Inorg. Chem.*, 2001, **40**, 4053–4062.
- 42 D. N. Kozhevnikov, V. N. Kozhevnikov, M. Z. Shafikov, A. M. Prokhorov, D. W. Bruce and J. A. G. Williams, *Inorg. Chem.*, 2011, **50**, 3804–3815.
- 43 Y. Liu, W. Wu, J. Zhao, X. Zhang and H. Guo, *Dalton Trans.*, 2011, **40**, 9085–9089.
- 44 Y. Liu, H. Guo and J. Zhao, *Chem. Commun.*, 2011, **47**, 11471–11473.
- 45 J. Zhao, S. Ji, W. Wu, W. Wu, H. Guo, J. Sun, H. Sun, Y. Liu, Q. Li and L. Huang, *RSC Adv.*, 2012, **2**, 1712–1728.
- 46 Y. Feng, J. Cheng, L. Zhou, X. Zhou and H. Xiang, *Analyst*, 2012, **137**, 4885–4901.
- 47 T. Yoshihara, Y. Yamaguchi, M. Hosaka, T. Takeuchi and S. Tobita, *Angew. Chem., Int. Ed.*, 2012, **51**, 4148–4151.
- 48 R. Ciriminna and M. Pagliaro, *Analyst*, 2009, **134**, 1531–1535.
- 49 H. Xiang, L. Zhou, Y. Feng, J. Cheng, D. Wu and X. Zhou, *Inorg. Chem.*, 2012, **51**, 5208–5212.
- 50 Y. Y. Cheng, B. Fückel, R. W. Macqueen, T. Khoury, R. G. C. R. Clady, T. F. Schulze, N. J. E. Daukes,

- M. J. Crossley, B. Stannowski, K. Lips and T. W. Schmidt, *Energy Environ. Sci.*, 2012, **5**, 6953–6959.
- 51 J. S. Lissau, J. M. Gardner and A. Morandeira, *J. Phys. Chem. C*, 2011, **115**, 23226–23232.
- 52 T. F. Schulze, J. Czolk, Y. Y. Cheng, B. Fückel, R. W. Macqueen, T. Khoury, M. J. Crossley, B. Stannowski, K. Lips, U. Lemmer, A. Colsmann and T. W. Schmidt, *J. Phys. Chem. C*, 2012, **116**, 22794–22801.
- 53 R. S. Khnayzer, J. Blumhoff, J. A. Harrington, A. Haeefe, F. Deng and F. N. Castellano, *Chem. Commun.*, 2012, **48**, 209–211.
- 54 Q. Liu, T. Yang, W. Feng and F. Li, *J. Am. Chem. Soc.*, 2012, **134**, 5390–5397.
- 55 S. M. Borisov, C. Larndorfer and I. Klimant, *Adv. Funct. Mater.*, 2012, **22**, 4360–4368.
- 56 R. R. Islangulov, D. V. Kozlov and F. N. Castellano, *Chem. Commun.*, 2005, 3776–3778.
- 57 W. Zhao and F. N. Castellano, *J. Phys. Chem. A*, 2006, **110**, 11440–11445.
- 58 W. Wu, H. Guo, W. Wu, S. Ji and J. Zhao, *Inorg. Chem.*, 2011, **50**, 11446–11460.
- 59 W. Wu, J. Zhao, H. Guo, J. Sun, S. Ji and Z. Wang, *Chem.–Eur. J.*, 2012, **18**, 1961–1968.
- 60 Q. Li, H. Guo, L. Ma, W. Wu, Y. Liu and J. Zhao, *J. Mater. Chem.*, 2012, **22**, 5319–5329.
- 61 W. Wu, S. Ji, W. Wu, J. Shao, H. Guo, T. D. James and J. Zhao, *Chem.–Eur. J.*, 2012, **18**, 4953–4964.
- 62 J. Sun, W. Wu and J. Zhao, *Chem.–Eur. J.*, 2012, **18**, 8100–8112.
- 63 X. Yi, J. Zhao, W. Wu, D. Huang, S. Ji and J. Sun, *Dalton Trans.*, 2012, **41**, 8931–8940.
- 64 W. Wu, J. Zhao, W. Wu and Y. Chen, *J. Org. Chem.*, 2012, **713**, 189–196.
- 65 H. Guo, Q. Li, L. Ma and J. Zhao, *J. Mater. Chem.*, 2012, **22**, 15757–15768.
- 66 Y. Y. Cheng, T. Khoury, R. G. C. R. Clady, M. J. Y. Tayebjee, N. J. E. Daukes, M. J. Crossley and T. W. Schmidt, *Phys. Chem. Chem. Phys.*, 2010, **12**, 66–71.
- 67 P. Yang, W. Wu, J. Zhao, D. Huang and X. Yi, *J. Mater. Chem.*, 2012, **22**, 20273–20283.
- 68 W. Wu, J. Zhao, J. Sun and S. Guo, *J. Org. Chem.*, 2012, **77**, 5305–5312.